Life Sciences 234 (2019) 116793

Contents lists available at ScienceDirect

Life Sciences

journal homepage: www.elsevier.com/locate/lifescie

Microbiota determines insulin sensitivity in TLR2-KO mice

Dioze Guadagnini[a,1], Guilherme Zweig Rocha[a,1], Andrey Santos[a], Heloisa Balan Assalin[a], Sandro Massao Hirabara[b], Rui Curi[b], Alexandre Gabarra Oliveira[a,c], Patricia O. Prada[d], Mario J.A. Saad[a,*]

[a] Department of Internal Medicine-FCM, University of Campinas-UNICAMP, Campinas, SP, Brazil.
[b] Interdisciplinary Post-Graduate Program in Health Science, Cruzeiro do Sul University, Sao Paulo, Brazil
[c] Department of Physical Education, Biosciences Institute, São Paulo State University (UNESP), Rio Claro, SP, Brazil
[d] Graduate Program in Nutritional and Sport Sciences and Metabolism, School of Applied Sciences, University of Campinas- UNICAMP, Campinas, Brazil

ARTICLE INFO

Keywords:
Gut microbiota
Insulin resistance
LPS
Genetic protection
TLR2

ABSTRACT

Introduction: Environmental factors have a key role in the control of gut microbiota and obesity. TLR2 knockout ($TLR2^{-/-}$) mice in some housing conditions are protected from diet-induced insulin resistance. However, in our housing conditions these animals are not protected from diet-induced insulin-resistance.
Aim: The aim of the present study was to investigate the influence of our animal housing conditions on the gut microbiota, glucose tolerance and insulin sensitivity in $TLR2^{-/-}$ mice.
Material and methods: The microbiota was investigated by metagenomics, associated with hyperinsulinemic euglycemic clamp and GTT associated with insulin signaling through immunoblotting.
Results: The results showed that $TLR2^{-/-}$ mice in our housing conditions presented a phenotype of metabolic syndrome characterized by insulin resistance, glucose intolerance and increase in body weight. This phenotype was associated with differences in microbiota in $TLR2^{-/-}$ mice that showed a decrease in the *Proteobacteria* and *Bacteroidetes* phyla and an increase in the *Firmicutes*phylum, associated with and in increase in the *Oscillospira* and *Ruminococcus* genera. Furthermore there is also an increase in circulating LPS and subclinical inflammation in $TLR2^{-/-}$. The molecular mechanism that account for insulin resistance was an activation of TLR4, associated with ER stress and JNK activation. The phenotype and metabolic behavior was reversed by antibiotic treatment and reproduced in WT mice by microbiota transplantation.
Conclusions: Our data show, for the first time, that the intestinal microbiota can induce insulin resistance and obesity in an animal model that is genetically protected from these processes.

1. Introduction

Although obesity and type 2 diabetes mellitus (T2DM) have genetic components, it is becoming clear that the environment also has a strong influence on the development of these metabolic disturbances, with the appearance of insulin resistance preceding the onset of these diseases [1–7]. In the past ten years, data from different sources have suggested that the gut microbiota plays a key causal role in obesity and insulin resistance [8–15]. Interestingly, the intestinal microbiota has been shown to be modulated by environmental factors, as well as host genetics [16,17], but recent evidence indicate that environment dominates over host genetics in shaping gut microbiota [18].

Previous data, from animal models and human studies, showed that the relative abundance of *Firmicutes* is higher in obese individuals, when compared to lean controls [19,20]. Furthermore, the gut microbiota can induce host insulin resistance through a variety of mechanisms, including: a) induction of systemic inflammation through Lipopolysaccharide (LPS) [21]; b) reduction of short chain fatty acids [22,23]; c) modulation of secondary biliary acids [24,25] and d) elevations in branched chain amino acids as well as other less well investigated mechanisms. While it is possible that these modulations are interdependent, the immune system is certainly involved in the

Abbreviations: KO, knockout; AKT, protein kinase B; GTT, glucose tolerance test; LPS, lipopolysaccharide; OTU, operational taxonomic unit; PBA, Phenyl Butyric Acid; MA, Monoassociated; NFκB, Nuclear factor kappa B; SOFA, Sequential Organ Failure Assessment; TLR2, Toll-like receptor 2; TLR4, Toll-like receptor 4; TNF-α, Tumor necrosis factor alpha; T2DM, Type 2 diabetes mellitus; UCP1, Uncoupling protein 1; PERK, protein kinase R (PKR)-like endoplasmic reticulum kinase

* Correponding author at: Rua Tessália Vieira de Camargo, 126 Cidade Universitária Zeferino Vaz, Campinas, SP 13084-971, Brazil.
E-mail address: msaad@fcm.unicamp.br (M.J.A. Saad).

[1] These authors contributed equally.

https://doi.org/10.1016/j.lfs.2019.116793
Received 21 May 2019; Received in revised form 17 August 2019; Accepted 25 August 2019
Available online 26 August 2019
0024-3205/ © 2019 Elsevier Inc. All rights reserved.

coordination of these mechanisms.

The innate immune system is an important regulator of the gut microbiota with pattern-recognition molecules, mainly Toll-like receptors (TLRs), having a central role in the process [26–28]. The seminal work of Vijay-Kumar et al. demonstrated that TLR5 deficient mice present hyperphagia and components of metabolic syndrome, including increased adiposity, hypertension and insulin resistance [29]. Interestingly, this study showed that this phenotype is secondary to alterations in the intestinal microbiota.

On the other hand, genetic and pharmacological TLR4 inactivation protects animals from high-fat diet-induced insulin resistance [30–35]. However, it appears as though the protective effect against diet-induced insulin resistance is independent of gut microbiota, since these mice are protected from this metabolic phenotype under different environmental and geographical conditions [26,27]. Similar to TLR4 KO mice, the genetic ablation of TLR2 also protects mice from insulin resistance induced by a high-fat diet [36–40]. However, in our housing conditions TLR2 KO mice ($TLR2^{-/-}$) gain more weight and are not protected from insulin resistance.

Since the environment has great influence on gut microbiota, which then modulates insulin action, it is expected a geographical variation in insulin sensitivity secondary to changes in the microbiota. In this regard, the aim of the present study was to investigate the influence that our animal housing conditions have on the gut microbiota, glucose tolerance and insulin sensitivity in $TLR2^{-/-}$.

2. Material and methods

2.1. Materials

Routine reagents were purchased from Sigma Chemical (St. Louis, MO, USA). The regular insulin was purchased from Eli Lilly (Indianapolis, Indiana, USA). Immunoblotting reagents were from Bio-Rad. Protein A- Sepharose 6 MB, nitrocellulose and chemiluminescence kits were from Amersham Biosciences (Little Chalfont, UK). Sense and antisense oligonucleotides specific for TLR4 (sense, 59-C TGA AAA AGC ATT CCC ACC T-39 and antisense, 59-A GGT GGG AAT GCT TTT TCA G-39) were synthesized by Invitrogen Corp. (Carlsbad, CA). The antibodies used in this study were obtained from Santa Cruz Biotechnology, Inc. (Santa Cruz, CA), Abcam (Cambridge, MA), or Cell Signaling Technology (Beverly, Massachusetts, USA), as depicted in figure legends of immunoblots.

2.2. Animals

Four week old male $TLR2^{-/-}$ and wild-type (WT) C57BL6/J mice were obtained (six to eight mice per group) from the University of Campinas Central Breeding Center and housed in a temperature controlled room (22 °C) under a 12/12 h light/dark cycle. This study was approved by the animal ethics committee and adhered to all of the university guideline recommendations pertaining to the use of animals in experimental studies. $TLR2^{-/-}$ and WT mice received water and food ad libitum throughout the experimental protocol.

2.3. Measurement of food intake

The mice were placed in individual metabolic cages (Tecniplast, Italy), and food intake was determined by measuring the difference between the amount of food provided and the amount of food remaining, during a 24-hour period, and averages were calculated over five days.

2.4. Hormones, cytokines and LPS serum determination

ELISA kits were utilized for the determination of serum insulin, leptin, adiponectina (Millipore, St Charles, MO, USA), TNF-α and IL-6 (ThermoFisher Scientific, Rockford, IL, USA) levels. While circulating LPS levels were measured using the commercially available Limulus Amebocyte Assay (Cambrex, Walkersville, MD, USA), according to the protocol of the manufacturer.

2.5. Glucose tolerance test

The glucose tolerance tests were performed on mice that were fasted for 6 h. To assess fasting glucose and insulin levels an unchallenged blood sample was taken, and then the animals were challenged with an injection of 20% glucose into the peritoneum. The glucose and insulin levels were assessed in tail blood samples, at 30, 60, 90 and 120 min after the challenge, as previously described [41,42].

2.6. Hyperinsulinemic–euglycemic clamp studies

Following a 6 h fasting period, mice were anesthetized and infused with insulin and glucose, through catheters inserted in the jugular vein. Another catheter was inserted into the femoral artery and used for collecting blood samples. A 120-minute hyperinsulinemic–euglycemic clamp was performed with a prime continuous infusion of regular insulin (3 mU/kg/min). Blood glucose was measured at 5-minute intervals, and glucose (10%) was infused at variable rates to maintain euglycaemia [43].

2.7. Tissue extraction, immunoprecipitation and protein analysis by immunoblotting

Mice, fasted overnight, were anesthetized with an intraperitoneal injection of sodium thiopental and the anesthetic depth and insensibility were assessed by the loss of pedal and corneal reflexes. Insulin (10 U) or saline solution was injected intraperitoneally. Then the liver and muscle were removed, coarsely minced and homogenized in lysis buffer at 4 °C. Lysates were processed as previously described [44]. Experiments utilizing immunopreciptation or immunoblotting were performed according to previously published work [45–47].

2.8. Metagenome profile

Fecal samples were collected, frozen in liquid nitrogen and stored at −80 °C until use. The genomic DNA was extracted using the QIAamp DNA Stool Mini Kit (Qiagen, Hilden, Germany). For each sample the V3–V4 hyper-variable region of the bacterial 16S rRNA gene was amplified followed by Illumina 16S Metagenomic Sequencing Library Preparation guide [48]. The Illumina Truseq DNA Sample Preparation v2 kit with bar code for each sample was used for the preparation of the libraries. The sequencing was performed in the Illumina Hiseq2000 equipment by the Central Laboratory of High Performance Technologies in Life Sciences (LaCTAD) of UNICAMP. The following Computational analysis tools were used in the analysis: FastQC; QIIME; OTU identification, with Greengenes reference OTUs (version 13.8).

2.9. Inhibition of ER stress

The animals were treated with Phenyl Butyric Acid (PBA) two times a day (500 mg/kg at each dose) by gavage for 10 consecutive days. This treatment protocol was adapted from Won et al. [49]. Untreated animals received the same volume of vehicle under the same treatment regime.

2.10. Evaluation of LPS absorption

Following a 6 h fast, mice were challenged with an oral dose of LPS (300 mg/kg) diluted in 100 mL of vehicle (water). Unchallenged animals received the same amount of water. LPS absorption was analyzed in blood samples that were collected, from the cava vein, 60 min after

the challenge. The plasma was separated and stored at -80 °C until use.

2.11. JNK inhibition

The potent and selective JNK inhibitor, SP600125, was prepared by making a 7% solution, in PBS, with Solutol HS-15 added as an emulsifying agent. Mice were injected with 30 mg/kg/day, for 5 days [50].

2.12. Antibiotics treatment

A mixture of antibiotics (ampicillin 1 g/L, metronidazole 1 g/L, vancomycin 0.5 g/L and neomycin 0.5 g/L) was added to the drinking water of 4 weeks old WT and TLR2$^{-/-}$ mice for 3 weeks. Throughout the duration of the experimental period, both food intake and stool microbiota were monitored.

2.13. Microbiota transplantation

The microbiota transplantation experiments were performed with pooled fecal content extracted from TLR2$^{-/-}$ or WT mice. The fecal extracts were suspended in PBS (1 fecal pellet of approximately 50 mg suspended in 1 mL of PBS) and immediately administered (0.2 mL per mouse) by gavage to 4 week old male mono-associated (MA) mice, colonized only with bacteria from the *Bacillus* genus, obtained from the Central Breeding Center at the State University of Campinas [51,52]. Microbiota transplanted mice were maintained in pathogen-free cages and monitored for body weight [29].

2.14. Statistical analysis

Data are expressed as means ± SD, and the number of mice is indicated. The immunoblot results are presented as direct comparisons of bands on acquired images, and quantified by optical densitometry (Chemidoc XRS+ from BIORAD, Hercules, CA, USA). For statistical analysis, all groups were compared using a Student's *t*-Test or one-way ANOVA with the Bonferroni test for post hoc comparisons. The level of significance adopted was $p < 0.05$.

3. Results

3.1. Animal characteristics

During the first 12 weeks of age, the average body weight of the TLR2$^{-/-}$ mice and control WT animals was similar. However, after 12 weeks, the body weight of the TLR2$^{-/-}$ mice began to increase (Fig. 1A). In accordance with this result, the epididymal fat weight was also similar in TLR2$^{-/-}$ mice and WT at 8 weeks of age, but was nearly two-fold higher in TLR2$^{-/-}$ mice at week 16 (Fig. 1B). To further investigate the cause of the observed increases in body and epididymal fat weight, we first measured the average daily food intake for WT and TLR2$^{-/-}$ mice. Food intake showed no observable differences between the WT and TLR2$^{-/-}$ mice at 8 weeks (WT = 5.05 ± 0.33 g/animal/day × TLR2$^{-/-}$ = 4.95 ± 0.41 g/animal/day) or 16 weeks (WT = 5.30 ± 0.42 g/animal/day × TLR2$^{-/-}$ = 5.23 ± 0.37 g/animal/day) of age.

Since no difference in food intake was observed, we next analyzed if energy expenditure could be responsible for the difference in the weight of TLR2$^{-/-}$ mice. For this, we observe that oxygen consumption in TLR2$^{-/-}$ mice is decreased when compared with WT mice (Fig. 1C), suggesting a decreased energy expenditure. We also verified if UCP1, a marker of thermogenesis, was altered in the brown adipose tissue of both group. TLR2$^{-/-}$ mice present a reduction in UCP1 when compared to WT mice (Fig. 1D), again suggesting a decrease in energy expenditure, corroborating the reduction in oxygen consumption.

Glucose tolerance and insulin sensitivity were evaluated in WT and TLR2$^{-/-}$mice, at 8 weeks of age, to determine if alterations in these parameters could be observed before the increase in adipose tissue. Interesting, at eight weeks of age the TLR2$^{-/-}$ mice presented a decrease in glucose tolerance (Fig. 1E), indicating that this abnormality was independent of body weight. Additionally, there was no significant difference in fasting insulin concentrations between WT and TLR2$^{-/-}$ mice (Fig. 1F). However, during the hyperinsulinemic-euglycemic clamp experiment, TLR2$^{-/-}$ mice displayed a significant decrease in the glucose infusion rate (a decrease of 50% of control, $p < 0.05$; Fig. 1G), thus characterizing the insulin resistance in these animals. The circulating levels of IL-6, TNF-α, leptin, and adiponectin were similar in WT and TLR2$^{-/-}$ mice (Fig. 1H-K). It should also be pointed out that the circulating levels of LPS were significantly higher in TLR2$^{-/-}$ mice, when compared to WT mice (Fig. 1L). Having confirmed the presence of insulin resistance in the TLR2$^{-/-}$ mice, it was then necessary to identify the molecular mechanism(s) that contribute to this phenotype.

3.2. Molecular mechanisms of insulin resistance

Western blot analyses of samples from liver and muscle of TLR2$^{-/-}$ mice indicated that the increase in insulin-induced IRβ tyrosine phosphorylation, the association of IRS-1/IRS-2 with p85 subunit of PI3 kinase and serine phosphorylation of AKT were blunted (Fig. S1A–C and Fig. 2A), which further confirmed this situation of insulin resistance. Due to the fact that TLR4 activation and subsequent downstream signaling events can antagonize insulin signaling, TLR4 activation was investigated in the liver and muscle by immunoprecipitating whole tissue extracts with an antibody against the combination TLR4-MyD88. The blots were then probed using an anti-TLR4 and anti-MyD88 antibodies, and showed that in the tissues of 8 week old TLR2$^{-/-}$ mice there was a clear association between TLR4 and Myd88 in liver and muscle (Fig. 2B and Fig. S2A), which is indicative of TLR4 activation. Regarding total protein amount, the results show an increase in TLR4 and MyD88 in TLR2$^{-/-}$ mice (Fig. S2B and C). There was also evidence of increased ER stress in the livers of TLR2$^{-/-}$ mice. In both the liver and muscle of TLR2$^{-/-}$ mice, there was an increase in JNK and c-jun phosphorylation, along with IRS-1 serine 307 phosphorylation, which provides evidence, at the molecular level, for insulin resistance (Fig. S3A, Fig. 2C and D). Concerning PERK phosphorylation levels, these were only found to be increased in the liver of TLR2$^{-/-}$ mice (Fig. 2E). We next investigated NFκB activation, using nuclear extracts from the liver and muscle. Surprisingly, there were no differences in the activation of this pathway between tissues from of TLR2$^{-/-}$ and WT mice (Fig. 2F). Since this pathway is downstream of TLR4 activation, this result suggests that in the absence of TLR2, TLR4 downstream signaling is not completely activated, but there is pathway specific activation, with JNK activation but not NFκB pathway.

Previous data showed that in obese mice the increase in circulating LPS is related to increased translocation of this lipid. We then investigated the increase in LPS in TLR2$^{-/-}$ was also related to an increase in translocation. Towards this goal, both WT and TLR2$^{-/-}$ mice were administered LPS by gavage, and then serum LPS levels were measured 2 h later. After 2 h, there was an increase in serum LPS concentration in both groups; however, a more marked increase was observed in the TLR2$^{-/-}$ mice, when compared to WT (Fig. 3A). Based on this result, it appears as though TLR2$^{-/-}$ mice have an increased gut permeability to LPS, which contributes to explaining why there are increased circulating levels of this lipid.

To investigate the role of TLR4 activation in insulin resistance in TLR2$^{-/-}$ mice, TLR4 activation was blocked with an antisense RNA to TLR4 (Fig. S4A). The antisense treated TLR2$^{-/-}$ animals showed higher glucose infusion during the euglycemic-hyperinsulinemic clamp when compared with the untreated TLR2$^{-/-}$ mice (Fig. 3B). The antisense treated animals also exhibited an improvement in insulin-induced AKT phosphorylation in liver (Fig. 3C).

With regards to JNK activation, this was investigated through pharmacological blockage of the activation. It was found that, after

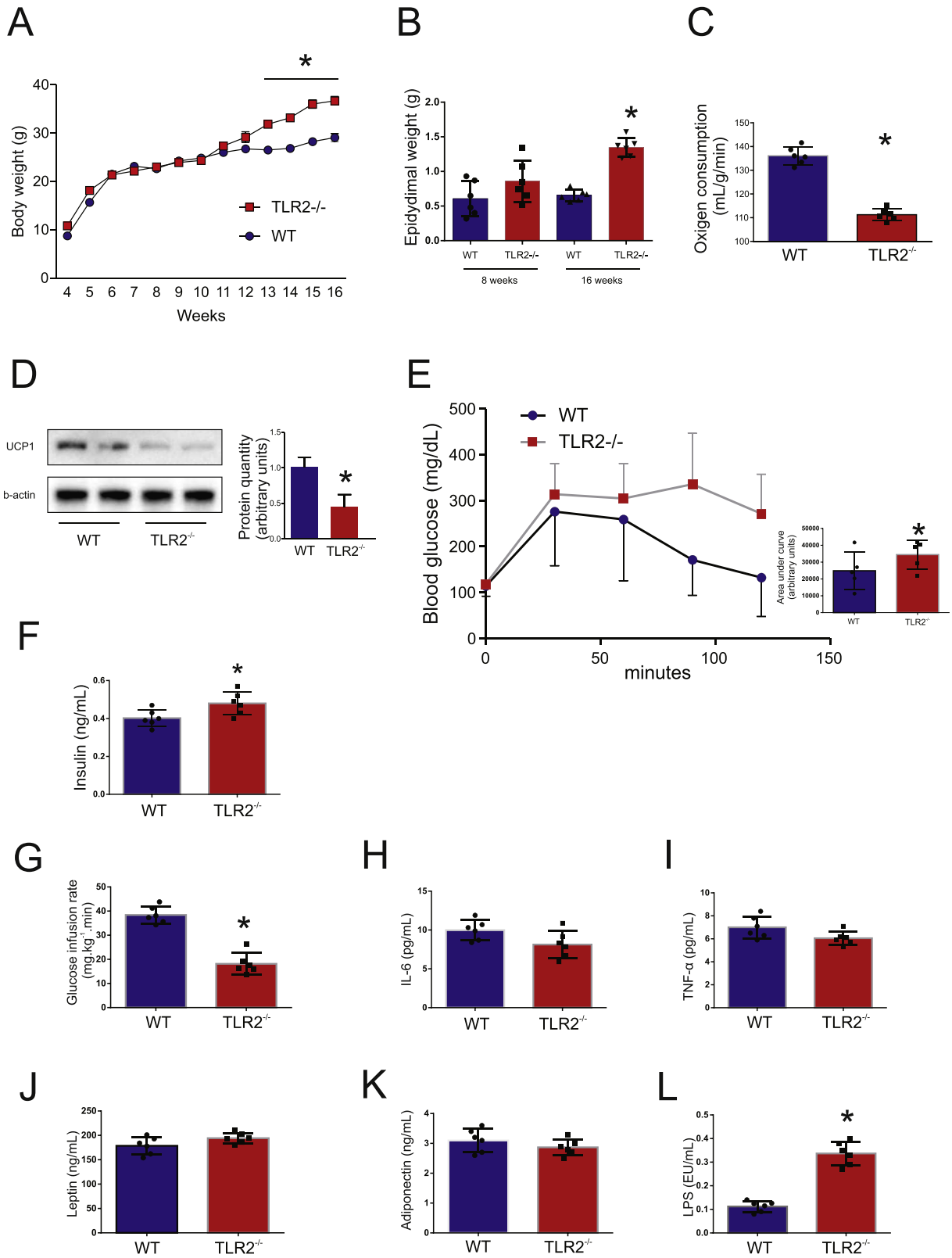

Fig. 1. TLR2$^{-/-}$ and WT mice metabolic characteristics.
(A) Weekly weight measurement from week 4 through 16 of age from TLR2$^{-/-}$ (red squares) and WT (blue circles) mice. (B) Epididymal fat pad weight at 8 and 16 weeks from TLR2$^{-/-}$ and WT mice. (C) Oxygen consumption (D) UCP-1 expression in the brown adipose tissue. (E) Blood glucose from TLR2$^{-/-}$ and WT mice during a glucose tolerance test (GTT) at 8 weeks of age. The inserted graph shows the area under the curve of the blood glucose during the GTT (arbitrary units). (F) Fasting serum insulin concentration in WT and TLR2$^{-/-}$ mice at 8 weeks of age. (G) Glucose infusion rate obtained from euglycaemic hyperinsunaemic clamp from TLR2$^{-/-}$ and WT mice at 8 weeks of age. (H) Serum concentration of IL-6, (I) TNF-α, (J) leptin, (K) adiponectin and (L) LPS from TLR2$^{-/-}$ and WT mice at 8 weeks of age. All evaluations were made with mice on standard chow. Data are presented as means ± S.D. from six to eight mice per group. *$p < 0.05$ between TLR2$^{-/-}$ mice and their controls. (For interpretation of the references to colour in this figure legend, the reader is referred to the web version of this article.)

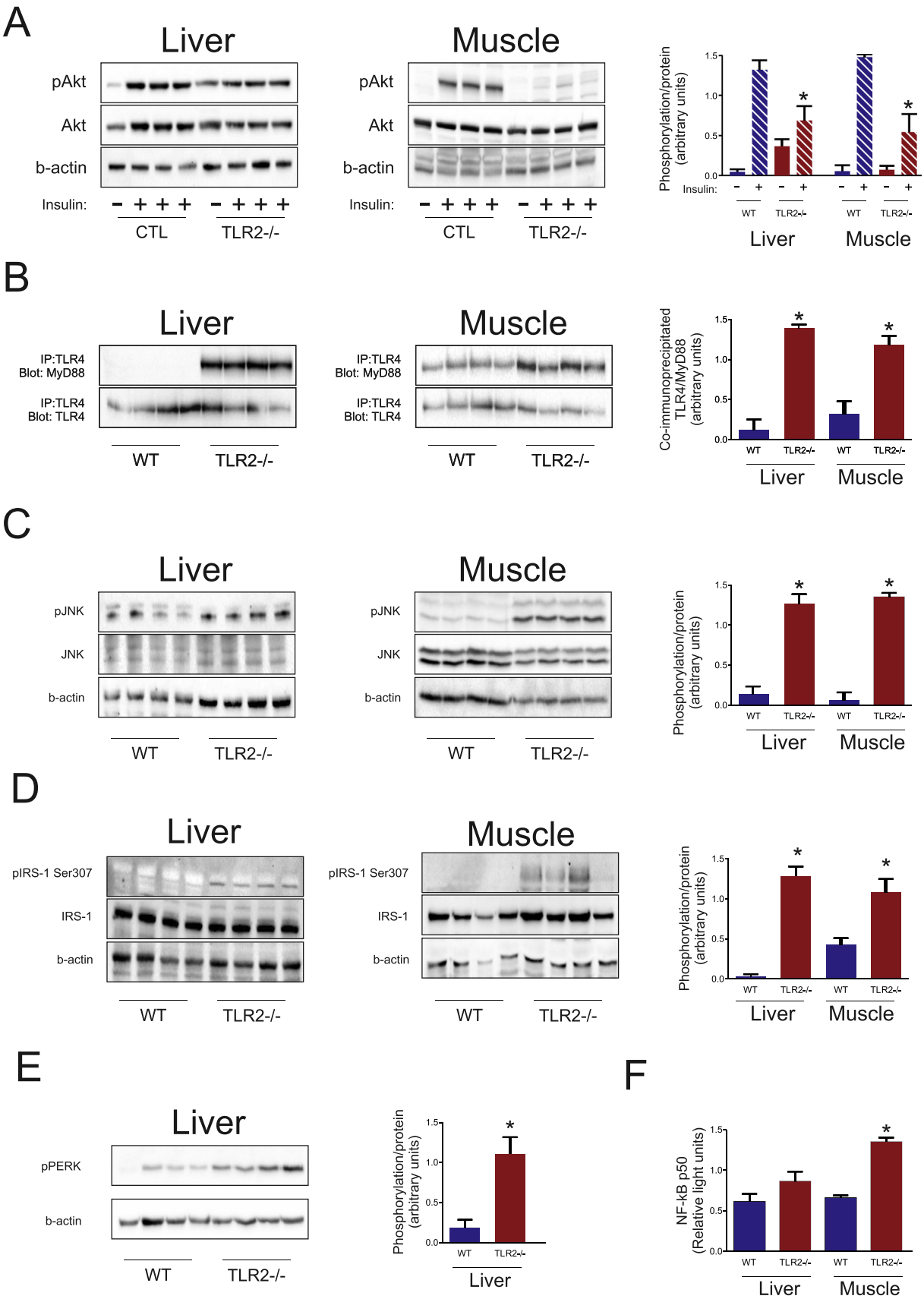

(caption on next page)

Fig. 2. Analysis of pathways involved insulin signaling impairment.
(A) Phosphorylation of serine 473 residue of Akt (antibody #9271 from CST) without insulin stimulation (-) or with 10U of intraperitoneal insulin injection (+) in liver (left panel) and muscle (middle panel) of TLR2$^{-/-}$ and WT mice. Akt (antibody #9272 from CST) and β -actin (antibody #4967 from CST) were measured as loading controls and the phosphorylation ratio to loading controls are shown in the graph (right panel). (B) Activation of TLR4 (studied by the immunoprecipitation of TLR4 (antibody SC-13593 from Santa Cruz Biotechnology) and blotted with MyD88 (antibody SC-11356 from Santa Cruz Biotechnology)) in liver (left panel) and muscle (middle panel) of TLR2$^{-/-}$ and WT mice. TLR4 (antibody #2219 from CST) was measured as loading controls and the activation of TLR4 are shown in the graph (right panel). (C) Phosphorylation of threonine 183 and tyrosine 185 residues of JNK (antibody SC-12882-R from Santa Cruz Biotechnology) in liver (left panel) and muscle (middle panel) of TLR2$^{-/-}$ and WT mice. JNK-1 (antibody SC-1648 from Santa Cruz Biotechnology) and β -actin (antibody #4967 from CST) were measured as loading controls and the phosphorylation ratio to loading controls are shown in the graph (right panel). (D) Phosphorylation of serine 307 residue of IRS-1 (antibody SC-33956 from Santa Cruz Biotechnology) in liver (left panel) and muscle (middle panel) of TLR2$^{-/-}$ and WT mice. IRS-1 (antibody SC-559 from Santa Cruz Biotechnology) and β -actin (antibody #4967 from CST) were measured as loading controls and the phosphorylation ratio to loading controls are shown in the graph (right panel). (E) Phosphorylation of threonine 980 residue of PERK (antibody #3179 from CST) in liver of TLR2$^{-/-}$ and WT mice. β -actin (antibody #4967 from CST) was measured as loading controls and the phosphorylation ratio to loading control are shown in the graph (right panel). (F) NFκB activation in nuclear extracts of liver and muscle of TLR2$^{-/-}$ and WT mice. All evaluations were made with mice on standard chow. Data are presented as means ± S.D. from six to eight mice per group. * $p < 0.05$ between TLR2−/− mice and their controls.

blockage with SP600125 (Fig. S4B), there was an increase in glucose uptake and insulin-induced AKT phosphorylation in the liver of TLR2$^{-/-}$ mice. This indicates that JNK activation, at least in TLR2$^{-/-}$ mice, is relevant in the progression of insulin resistance (Fig. 3C).

It is also possible that JNK activation may be consequence of ER stress in the liver cells. To test this hypothesis ER stress was inhibited with PBA, and resulted in improved glucose infusion during the clamp and increased Akt phosphorylation levels in the livers of TLR2$^{-/-}$ mice, following insulin stimulation (Fig. 3C).

3.3. Gut microbiota composition in TLR2$^{-/-}$ mice

To investigate how TLR2$^{-/-}$ genotype affected the microbiota phylogenetic richness, we analyzed the α-diversity, as assessed by rarefication and phylogenetic diversity. The number of OTUs and Faith's Phylogenetic Diversity in the WT group were significantly higher than in the TLR2$^{-/-}$ Group ($p = 0.004$) (Fig. 4A). The unweighted UniFrac distance was used to compare bacterial composition of microbiota between WT and TLR2$^{-/-}$, resulting in a spatial separation between groups. PERMANOVA detected significant differences in the gut microbiota among the groups ($p = 0.001$; Pseudo-F 12.045); (Fig. 4B). Statistically significant dissimilarities were observed between WT and TLR2$^{-/-}$ with respect to bacteria β-diversity (p = 0.001). Significant modifications in phyla and genera level between WT and TLR2$^{-/-}$ were shown by the Galaxy software [53]. The Linear Discriminant Analysis (LDA) and Effect Size (LEfSe) were also used to characterize the differences between biological conditions. It should be emphasized that major differences were observed such as Bacteroidetes and Protebacteria phyla and *Lactobacillus* and *Bifidobacterium* genera were increased in WT group, while the Firmicutes phylum and *Ruminococcus* and *Oscillospira* genera were increased in TLR2$^{-/-}$ group.

3.4. Administering antibiotics to TLR2$^{-/-}$ mice alters gut microbiota and improves insulin sensitivity

Since it is well known that antibiotics can modulate gut microbiota, a cocktail of antibiotics (ampicillin 1 g/L, metronidazole 1 g/L, vancomycin 0.5 g/L and neomycin 0.5 g/L) was added to the drinking water of TLR2$^{-/-}$ mice for 3 weeks. This association of antibiotics has broad spectrum and dramatically reduces gut microbiota. After this treatment, we analyzed the microbiota composition in the cecal content of the TLR2$^{-/-}$ mice. The Faith's Phylogenetic Diversity in the **TLR2**$^{-/-}$ + AB group was significantly different from WT group ($p = 0.003$) (Fig. 4A). However, the unweighted UniFrac distance was used to compare bacterial composition of microbiota between groups, resulting in a spatial separation between TLR2$^{-/-}$group and other groups, but not between WT and WT + AB group. (PERMANOVA detected significant differences in the gut microbiota among the TLR2$^{-/-}$ + AB and TLR2$^{-/-}$ $p = 0.031$; Pseudo-F 6.93); (Fig. 4B). Statistically significant dissimilarities were observed between TLR2$^{-/-}$ + AB and TLR2$^{-/-}$ with respect to bacteria β-diversity (p = 0.031). There were alterations in the relative abundance of three phyla of bacteria. There was a decrease in the abundance of *Bacteroidetes* and*Proteobacteria*, and a dramatic increase in the abundance of *Firmicutes* in these mice (Fig. 4C). Furthermore, the antibiotic treated TLR2$^{-/-}$ mice showed different profiles of bacterial genera (Fig. 5A).

The antibiotic treatment also resulted in a reduction of both epididymal and visceral fat weight in TLR2$^{-/-}$ mice (Fig. 5B and C) without a significant change in food intake (TLR2$^{-/-}$ 5.16 ± 0.36 g/animal/day; TLR2$^{-/-}$ AB 4.98 ± 0.31 g/animal/day). Additionally, it should be pointed out that these parameters were not altered in either the treated or the untreated WT mice (Fig. 5B and C WT 5.18 ± 0.33 g/animal/day; WT AB 4.99 ± 0.36 g/animal/day). Antibiotic-treated TLR2$^{-/-}$ mice also presented an amelioration in insulin resistance, as evidenced by increased glucose tolerance (Fig. 5D), glucose infusion rate during the euglycaemic-hyperinsulinaemic clamp (Fig. 5E) and insulin-stimulated Akt phosphorylation in the liver (Fig. 5F). On the other hand, we did not observe any differences in these parameters when comparing treated and untreated WT mice (Fig. 5D–F). Accordingly, the antibiotic treatment induced a significant reduction of the inflammation in liver and muscle in TLR2$^{-/-}$ mice, as evidenced by lower association of TLR4/MyD88 and phosphorylation levels of JNK and PERK (Fig. S5).

We then indirectly assessed the effects of antibiotic treatment on the intestinal integrity, through the detection of ZO-1 in the colon. The TLR2$^{-/-}$ mice had diminished ZO-1 content and AB treatment increased the expression of this protein to levels similar of control, and no significant alteration was observed in WT animals (Fig. 5G). Together, these data indicate that the changes in the gut microbiota of TLR2$^{-/-}$ mice, induced by AB, reversed the insulin resistance and glucose intolerance of these animals.

3.5. Transplanting TLR2$^{-/-}$ microbiota to Monoassociated (MA) mice increases weight gain and impairs insulin signaling

To further evaluate and confirm the important role of gut microbiota in the early steps of insulin resistance development in TLR2$^{-/-}$ mice, we carried out microbiota transplantation studies in four week old MA mice, colonized only with the *Bacillus* genus. When WT microbiota were transplanted into MA mice, while there was a trend in increasing body and epididymal fat weights, no significant alterations were observed; however, there was a significant increase in the relative amount of visceral adipose tissue observed (Fig. 6A–C). On the other hand, the body weight, relative epididymal fat, and visceral adipose tissue were all significantly increased when TLR2$^{-/-}$ microbiota were transplanted into MA (Fig. 6A–C). Additionally, a slight impairment in insulin sensitivity was observed in mice transplanted with the WT microbiota, while a major impairment was observed in mice that were transplanted with TLR2$^{-/-}$ microbiota, as evidenced by a large reduction in the glucose infusion rate, along with increased blood glucose

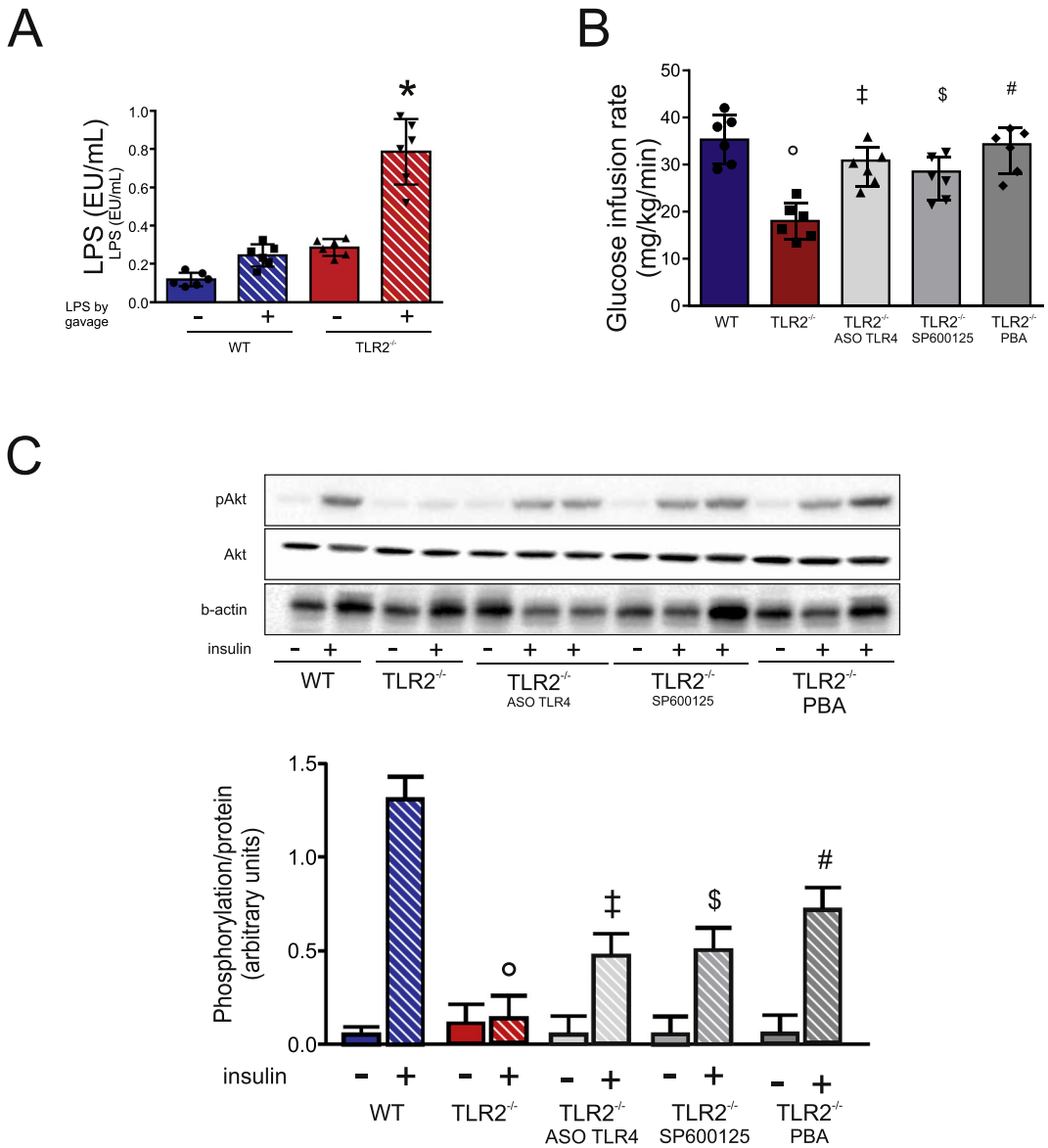

Fig. 3. Insulin sensitivity and signaling after treatment with selective inhibitors.
(A) LPS measurement in the serum of fasted TLR2$^{-/-}$ and WT mice gavaged with LPS (1.08 10^{-8} g) diluted in 100 μL of water (+) or with 100 μL of water without LPS (-). Blood was collected from the cava vein 60 min after gavage and serum LPS was determined. (B) Glucose infusion rate obtained by the euglycaemic hyperinsulinaemic clamp from WT mice and TLR2$^{-/-}$ mice treated or not with the drugs: JNK inhibitor, SP600125 (SP); endoplasmic reticulum stress inhibitor, 4-phenil butyric acid (PBA); and TLR4 antisense oligonucleotide (ASO). (C) Phosphorylation of serine 473 residue of Akt (antibody #9271 from CST) after the treatment with SP600125, PBA and ASO without insulin stimulation (-) or with 10 U of intraperitoneal insulin injection (+) in liver of TLR2$^{-/-}$ and WT mice. Akt (antibody #9272 from CST) and β -actin (antibody #4967 from CST) were measured as loading controls and the phosphorylation ratio to loading controls are shown in the graph below. All evaluations were made with mice on standard chow. Data are presented as means ± S.D. from six to eight mice per group from. *$p < 0.05$ in WT and TLR2−/− mice with LPS stimulus. ° $p < 0.05$ betweem WT and TLR2−/− mice; § $p < 0.05$ between TLR2−/− mice treated or not with ASO; $ $p < 0.05$ between TLR2−/− mice, treated or not with SP; # $p < 0.05$ between TLR2−/− mice with, treated or not with PBA.

and AUC during the GTT (Fig. 6D and E).

4. Discussion

The results of the present study show that under our animal housing conditions, the TLR2$^{-/-}$ mice fed a standard chow diet develop insulin resistance and glucose intolerance early and then gain more weight than controls. These phenotypic characteristics are secondary to changes in the gut microbiota, as shown by an increase in the phylum *Firmicutes* and a decrease in *Bacteroidetes*. The molecular mechanisms of insulin resistance in these animals involve an increase circulating LPS associated with TLR4/JNK activation, liver ER stress and insulin signaling downregulation in the liver and muscle. These alterations were present in 8 week old TLR2$^{-/-}$ mice, and precede the development of obesity, which was only observed after the 12 weeks of age, thus reinforcing the cause and effect relationship between intestinal microbiota modulation and increased body weight. Interestingly, the presence of insulin resistance before a detectable increase in adiposity has also been demonstrated in other animal models of obesity [54,55].

These results are in contrast with previous data that showed that TLR2$^{-/-}$ mice fed a HFD displayed less weight gain and adiposity, and did not develop insulin resistance, when compared to controls [36–40]. It is possible that gut microbiota may account for these differences. Although our TLR2$^{-/-}$ animals have the same genetic defect as described in other studies [36,37], our animals have different housing conditions, environments and food sources, which can all impact and

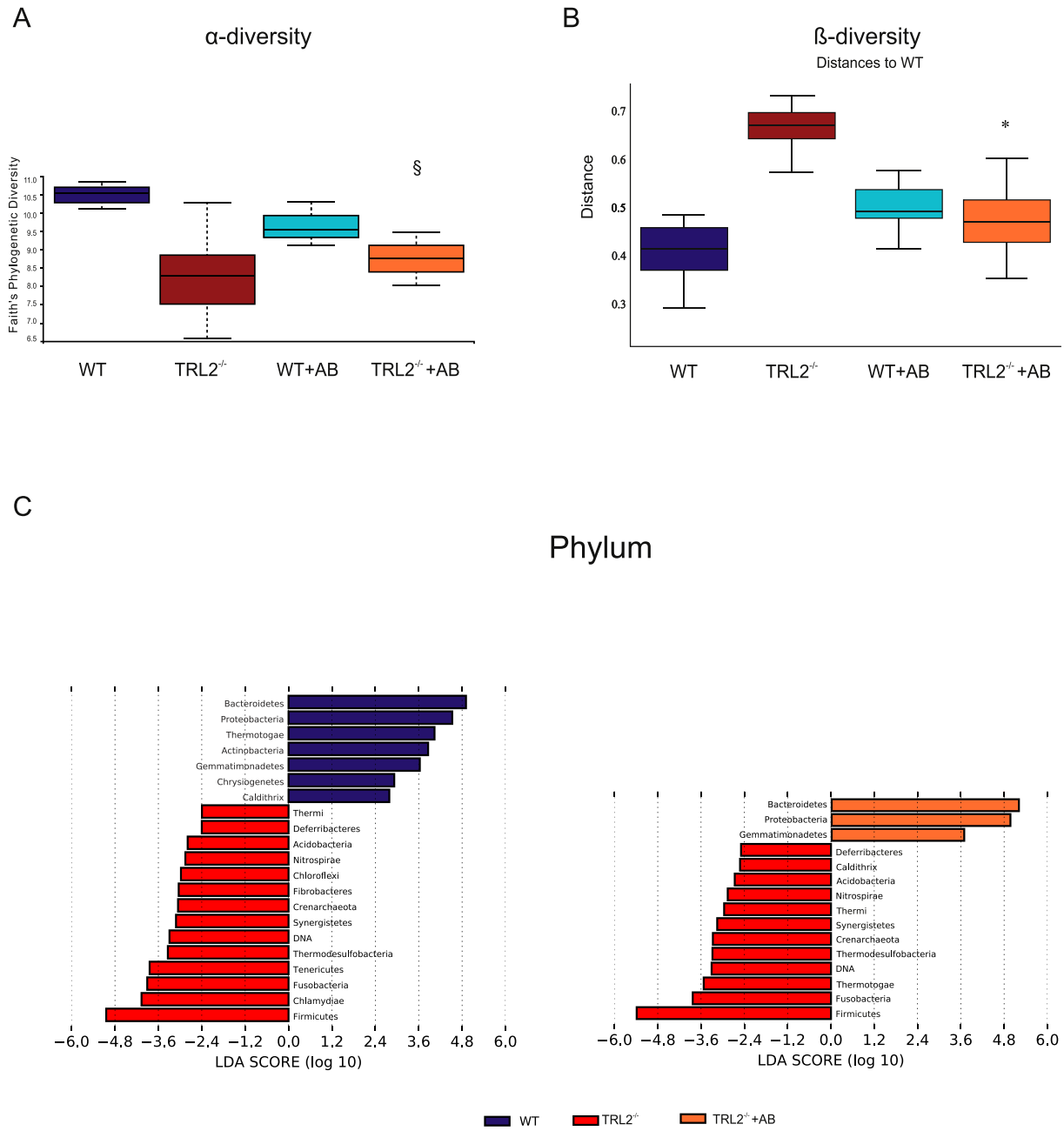

Fig. 4. Gut Microbiota Composition (A) Faith's Phylogenetic Diversity in the WT group and the TRL2$^{-/-}$ group treated or not with antibiotics. ($p = 0.004$); (B) The unweighted UniFrac distance was used to compare bacterial composition of microbiota among WT and TRL2−/− ($p = 0.001$; Pseudo-F 12.045); (C) Linear discriminant analysis (LDA) effect size indicated differences in phyla and genera between groups WT and TRL2−/− groups (taxa with LDA score > 2 and significance of a < 0.05 determined by Wilcoxon signed-rank test).

modify the gut microbiota. In this regard, at least one previous study investigated the microbiota in TLR2$^{-/-}$ mice and showed that the proportion of *Firmicutes* was lower and *Bacteroidetes* higher compared with our animals [56]. Furthermore, in our conditions the genera *Oscillospira* and *Ruminococcus* were higher in TLR2$^{-/-}$ animals and previous data showed that these genera are associated with adiposity and metabolic dysfunction, gut inflammation and serum tryglicerides in mice and humans [57–60].

It is important to mention that at least two key studies demonstrated that the microbiota could account for the metabolic syndrome phenotype. The first study showed that TLR5$^{-/-}$develops insulin resistance and hyperphagia associated obesity [29] secondary to changes in the composition of the gut microbiota. The second study utilized three inbred strains of mice to show that the development of metabolic syndrome and obesity is the result of interactions among host genetics, diet and gut microbiota [61]. In this regard, our study is unique, because it shows that in mice genetically protected from insulin resistance (TLR2$^{-/-}$), the microbiota could overcome this protection and still induce insulin resistance and obesity.

A plausible molecular mechanism by which microbiota modulation can induce insulin resistance is through an increase in circulating LPS levels. In fact, TLR2$^{-/-}$ mice presented elevated LPS levels, despite being fed standard rodent chow. This increase may be a consequence of changes in the microbiota and/or altered intestinal permeability. The genus *Blautia* was increased in TLR2$^{-/-}$ and a recent study showed that this genus could be positively correlated with increased intestinal permeability and secretion of inflammatory cytokines [62–64]. *Proteobacteria* and *Bacteroidetes* are the main sources of LPS, and these phyla

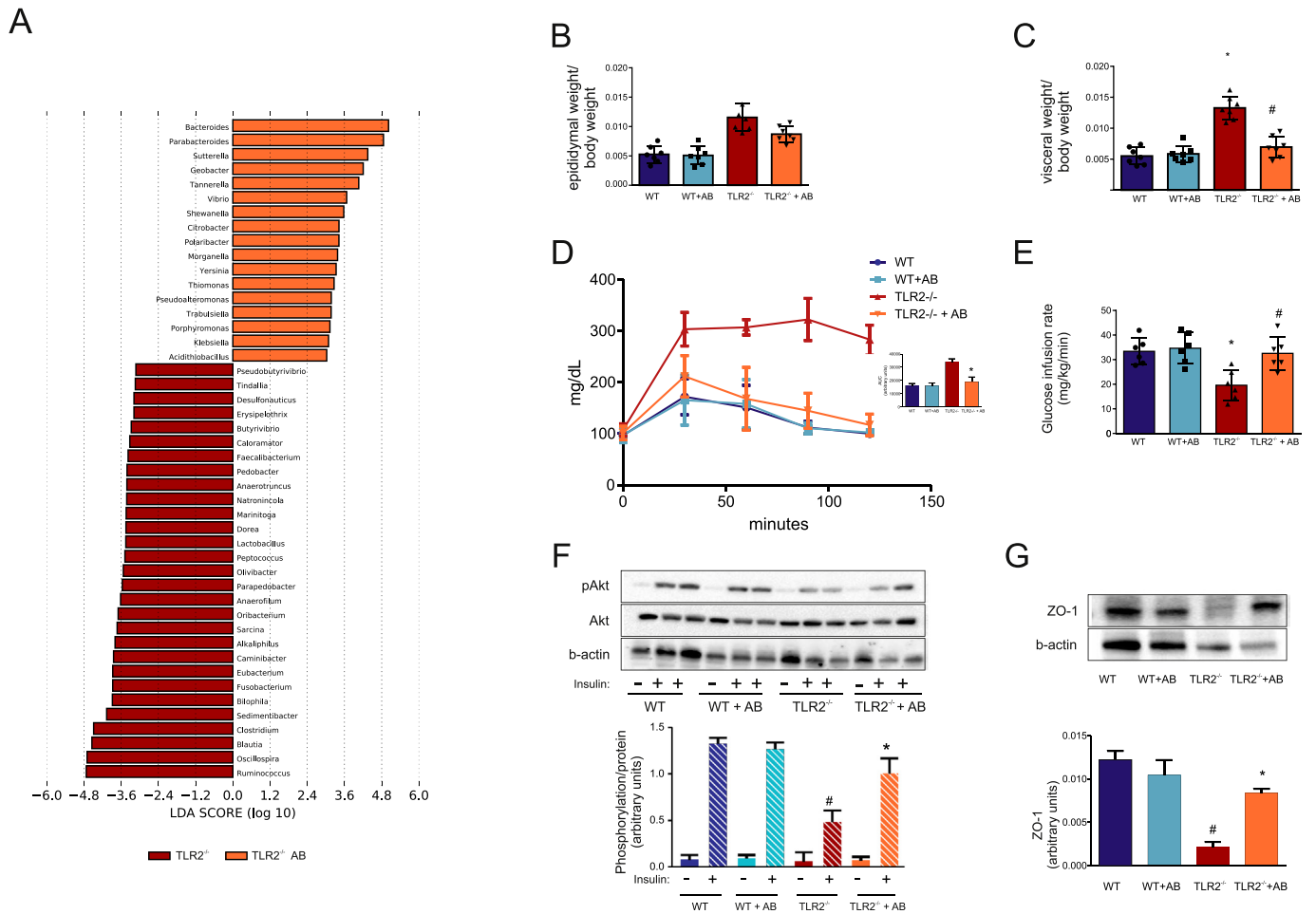

Fig. 5. Antibiotic treatment alter microbiota composition, the metabolic parameters and in insulin sensitivity and signaling in TLR2$^{-/-}$ mice. (A Linear discriminant analysis (LDA) effect size indicated differences in genera between groups TLR2−/− mice treated with vehicle or antibiotics (AB) (taxa with LDA score > 2 and significance of a < 0.05 determined by Wilcoxon signed-rank test). (B) Relative epidydimal fat pad weight of WT and TLR2$^{-/-}$ mice treated with vehicle or antibiotics (AB). (C) Relative visceral adipose tissue weight of WT and TLR2$^{-/-}$ mice treated with vehicle or antibiotics (AB). (D) Blood glucose from TLR2$^{-/-}$ and WT mice treated with antibiotics (AB) or vehicle during a glucose tolerance test (GTT). The inserted graph shows the area under the curve of the blood glucose during the GTT (arbitrary units). (E) Glucose infusion rate obtained from euglycaemic hyperinsunaemic clamp from TLR2$^{-/-}$ and WT mice treated with antibiotics (AB) or vehicle. (G) Phosphorylation of serine 473 residue of Akt (antibody #9271 from CST) in liver of WT or TLR2$^{-/-}$ mice after the treatment with antibiotics (AB) or vehicle without insulin stimulation (-) or with 10 U of intraperitoneal insulin injection (+) Akt (antibody #9272 from CST) and β -actin (antibody #4967 from CST) were measured as loading controls and the phosphorylation ratio to loading controls are shown in the graph below. (G) Zonula occludens (ZO)-1 (antibody SC-10804 from Santa Cruz Biotechnology) expression in the ileum of WT or TLR2$^{-/-}$ mice after the treatment with antibiotics (AB), and β -actin (antibody #4967 from CST) was measured as loading control and the ratio of ZO-1 over β-actin is shown in the graph below. Data are presented as means ± S.D. from six to eight mice per group. All evaluations were made with mice on standard chow. * $p < 0.05$ between TLR2−/− and TLR2−/− treated with AB; # $p < 0.05$ between WT mice; * $p < 0.05$ between WT and TLR2−/− mice.

are decreased in TLR2$^{-/-}$ mice, suggesting that the alteration in intestinal permeability is the main cause of this increase. Confirming the altered gut permeability in TLR2$^{-/-}$ mice the administration of LPS by gavage increased circulating levels of this lipid in TLR2$^{-/-}$ mice.

In accordance with this alteration in gut permeability, the TLR2$^{-/-}$ mice also displayed a decrease in the presence of colonic ZO-1 protein. It is important to point out that previous studies have shown that TLR2 functions as an important regulator of tight junction (TJ) and epithelial barrier integrity [65,66]. In this regard, in addition to this genetic predisposition to altered intestinal permeability, the changes in microbiota identified in our colony of TLR2$^{-/-}$ mice may also contribute to this barrier function alteration. This is further supported by the fact that the antibiotic cocktail reduced the intestinal microbiota, which was accompanied by an improvement in intestinal permeability. In accordance, Kellermayer et al. demonstrated that the microbiota also have an important role in the control of intestinal permeability [56].

Overall, TLR2$^{-/-}$ mice treated with antibiotics displayed reduced insulin resistance, circulating LPS levels and JNK and IRS-1ser307 phosphorylation, and increased insulin signaling in the liver and muscle. Thus, indicating the important role of the microbiota in the induction of insulin resistance in these animals. This role is further highlighted when it was shown that the transplantation of gut microbiota from TLR2$^{-/-}$mice to host WT MA (*Bacillus*-associated) mice induced weight gain, reduced glucose tolerance and insulin sensitivity/signaling, characteristics consistent with host insulin resistance. Taken together the antibiotic treatment and transplantation results suggest that the microbiota of TLR2$^{-/-}$ mice play a key role in changing the intestinal epithelial barrier integrity and/or function and increasing LPS circulating levels associated with insulin resistance.

The molecular mechanism by which the increase in LPS induced insulin resistance in TLR2$^{-/-}$ mice is unique and deserves analysis. We found that activation of TLR4/JNK was associated with an increase in IRS-1ser307 phosphorylation in tissues, which induces insulin resistance. Moreover, in addition to antibiotics, there was an

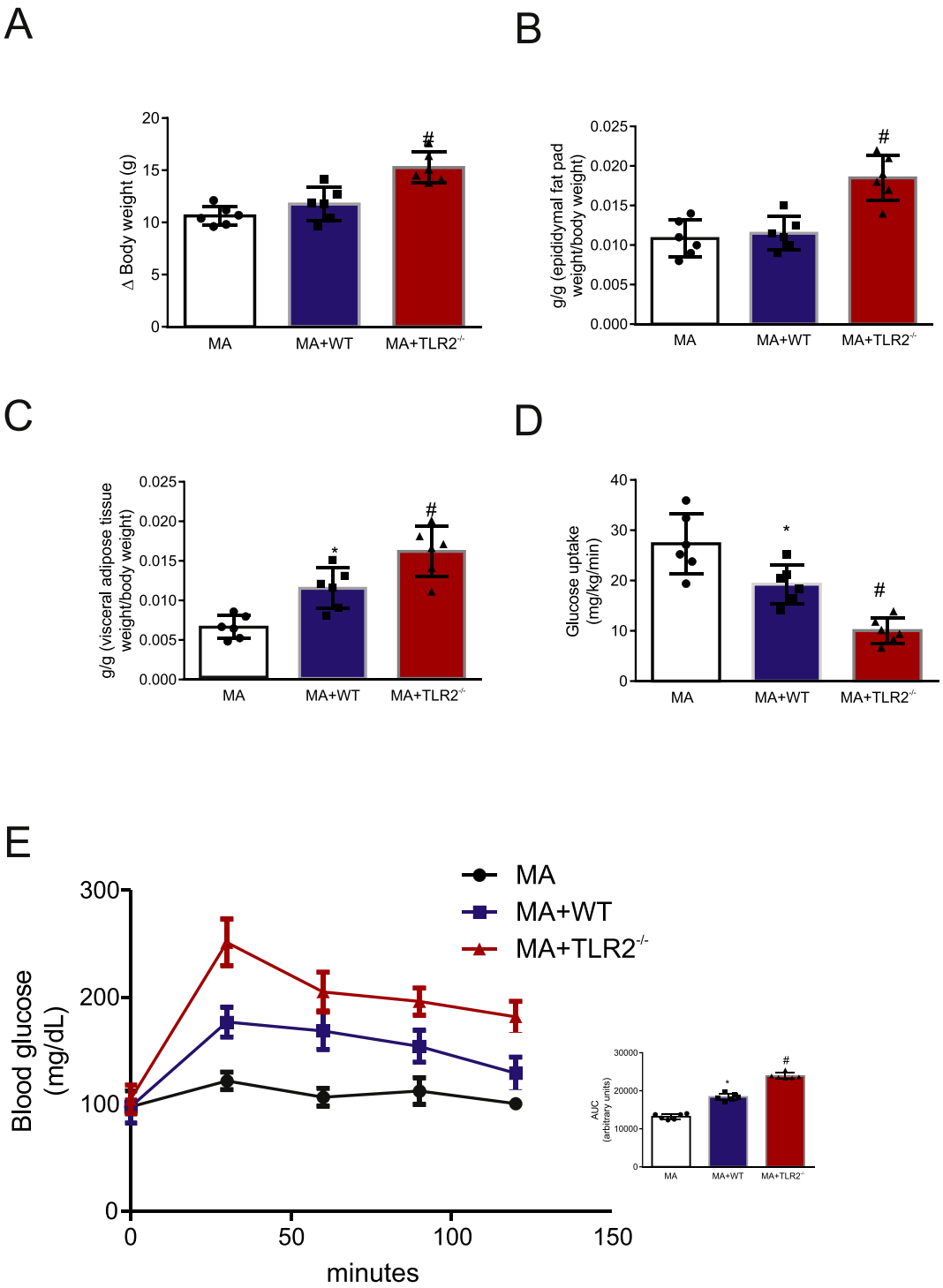

Fig. 6. Microbiota transplantation from TLR2$^{-/-}$ to WT Bacillus-associated mice increases weight gain and impairs insulin sensitivity.
(A) Body weight variation of WT Bacillus-associated (MA) mice, of WT Bacillus-associated mice transplanted with WT microbiota (MA + WT) and WT Bacillus-associated mice transplanted with TLR2$^{-/-}$ microbiota (MA + TLR2$^{-/-}$). (B) Relative epididymal fat pad weight of MA, MA + WT and MA + TLR2$^{-/-}$ mice. (C) Relative visceral adipose tissue weight of MA, MA + WT and MA + TLR2$^{-/-}$ mice. (D) Glucose infusion rate obtained from euglycaemic hyperinsunaemic clamp from MA, MA + WT and MA + TLR2$^{-/-}$ mice. (E) Blood glucose from MA, MA + WT and MA + TLR2$^{-/-}$ mice during a glucose tolerance test (GTT). The inserted graph shows the area under the curve of the blood glucose during the GTT (arbitrary units). Data are presented as means ± S.D. from six to eight mice per group. All evaluations were made with mice on standard chow. * $p < 0.05$ between *Bacillus*-associated mice transplanted with TLR2 − / − microbiota (MA + TLR2 − / −) and those transplanted with WT microbiota (MA + WT); # $p < 0.05$ between *Bacillus*-associated mice transplanted with WT microbiota (MA + WT) and *Bacillus*-associated mice (MA).

improvement in insulin resistance observed in these animals after treatment with PBA (blocker of ER stress), JNK blocker and TLR4 inactivation. We can then propose that the mechanism of insulin resistance in these animals begins with a modulation of the gut microbiota, which leads to an increase in circulating LPS levels, activating TLR4 and increasing JNK activation. In the liver, the JNK activation

may be a consequence, at least in part, of ER stress, which can also contribute to the development of insulin resistance. It is important to mention that the TLR4 activation in the TLR2$^{-/-}$ animals shows a different pattern of signaling compared to obesity. Usually in high-fat diet induced-insulin resistance and in obesity and type 2 diabetes there is a well characterized inflammatory process [67–69] associated with the activation of both JNK and NFkB pathways [30,35,43]. However, in TLR2 KO mice the insulin resistance is only characterized by JNK activation in liver and muscle, without any increase in TNF-α and IL-6 production, pointing for a unique molecular mechanism for the insulin resistance in these mice. The reason for this specific activation induced by LPS is not well established, but may involve a cooperation between TLR2 and TLR4 [70,71]. Laflamme et al. [70] showed that the first bolus of LPS injection in TLR2 KO mice induced genes encoding innate immune proteins, however, a second bolus failed to increase TNF-α, indicating that TLR2 is involved in the second wave of TNF-α expression through NFkB activation. We can thus speculate that in our TLR2$^{-/-}$ mice there is a similar pattern, in which the chronic increase in LPS activated JNK but failed to induce NFkB activation in tissues of these mice, suggesting the necessity of the cooperation between these two receptors for the complete activation by LPS.

Our results demonstrate that the relationships between gut microbiota, environment and host genetics are complex. The microbiota may interact in different ways with the host, depending on the genetic background, diet and environmental factors that cause changes in the microbiome as a consequence of the impact generated on host metabolism [61,72,73]. It is important to highlight that we could demonstrate by different methods, i.e. through antibiotic treatment and microbiota transplantation the influence of microbiota on the development of obesity, even in an animal model of genetic protection against insulin resistance. However, it is difficult to directly translate our results to human situations mainly because the intestinal microbiota of mice is different from men [74].

In summary, the results of the present study showed that TLR2$^{-/-}$ mice develop insulin resistance and gain body weight on a standard chow diet, which was associated with glucose intolerance, under our animal housing conditions. It was determined that these phenotypic characteristics are secondary to changes in the gut microbiota, and are associated with changes in the integrity of the intestinal epithelial barrier and increased circulating levels of LPS. The molecular mechanisms involved in insulin resistance observed in these animals are unique, and secondary to increased TLR4/JNK activation, elevated ER stress in the liver and downregulated insulin signaling in the liver and muscle, but not IKK/IκB/NF-κB pathway activation. The results from this study reinforce the importance of intestinal microbiota in the development of obesity and insulin resistance, and shows, for the first time, that intestinal microbiota can induce insulin resistance and obesity in an animal model genetically protected against these pathophysiological conditions.

Supplementary data to this article can be found online at https://doi.org/10.1016/j.lfs.2019.116793.

Ethics approval

All animal protocols of this study were approved by the Animal Care and Use Committee at State University of Campinas and they are guided by international guidelines for the care and use of experimental animals.

Availability of data and material

The datasets used and/or analyzed during the current study are available from the corresponding author on reasonable request.

Declaration of competing interests

The authors declare that they have no competing interests.

Funding

We also acknowledge the financial support INCT de Obesidade e Diabetes 465693/2014-8 (FAPESP) and CAPES/CNPq (Conselho Nacional de Desenvolvimento Científico e Tecnológico).

Authors' contributions

DG; GZR: researched data, contributed to discussion, wrote/reviewed/edited manuscript;

HBA; AS; AGO.: researched data, wrote/reviewed/edited manuscript;

SMH; RC; POP; M.J.A.S.: contributed to discussion, wrote/reviewed/edited manuscript.

Acknowledgements

The authors thank L. Janeri, *in memorium* (Department of Internal Medicine, UNICAMP, Campinas, São Paulo) and J. Pinheiro (Department of Internal Medicine, UNICAMP, Campinas, São Paulo) for their technical assistance.

References

[1] P. Hossain, et al., Obesity and diabetes in the developing world—a growing challenge, N. Engl. J. Med. 356 (3) (2007) 213–215.
[2] M.A. Lazar, How obesity causes diabetes: not a tall tale, Science 307 (5708) (2005) 373–375.
[3] A. Doria, et al., The emerging genetic architecture of type 2 diabetes, Cell Metab. 8 (3) (2008) 186–200.
[4] T. Rankinen, et al., The human obesity gene map: the 2005 update, Obesity (Silver Spring) 14 (4) (2006) 529–644.
[5] A.J. Walley, et al., The genetic contribution to non-syndromic human obesity, Nat Rev Genet 10 (7) (2009) 431–442.
[6] C. He, et al., High-fat diet induces dysbiosis of gastric microbiota prior to gut microbiota in association with metabolic disorders in mice, Front. Microbiol. 9 (2018) 639.
[7] K.E. Bouter, et al., Role of the gut microbiome in the pathogenesis of obesity and obesity-related metabolic dysfunction, Gastroenterology 152 (7) (2017) 1671–1678.
[8] P.D.A.J. Cani, M.A. Iglesias, M. Poggi, C. Knauf, D. Bastelica, A.M. Neyrinck, F. Fava, K.M. Tuohy, C. Chabo, A. Waget, E. Delmee, B. Cousin, T. Sulpice, B. Chamontin, J. Ferrieres, J.F. Tanti, G.R. Gibson, L. Casteilla, N.M. Delzenne, M.C. Alessi, R. Burcelin, Metabolic endotoxemia initiates obesity and insulin resistance, Diabetes (2007) 11.
[9] P.D. Cani, et al., Changes in gut microbiota control metabolic endotoxemia-induced inflammation in high-fat diet-induced obesity and diabetes in mice, Diabetes 57 (6) (2008) 1470–1481.
[10] S.J. Creely, et al., Lipopolysaccharide activates an innate immune system response in human adipose tissue in obesity and type 2 diabetes, Am. J. Physiol. Endocrinol. Metab. 292 (3) (2007) E740–E747.
[11] S. Chung, et al., Preadipocytes mediate lipopolysaccharide-induced inflammation and insulin resistance in primary cultures of newly differentiated human adipocytes, Endocrinology 147 (11) (2006) 5340–5351.
[12] P.J. Pussinen, et al., Endotoxemia is associated with an increased risk of incident diabetes, Diabetes Care 34 (2) (2011) 392–397.
[13] L.L. Stoll, et al., Potential role of endotoxin as a proinflammatory mediator of atherosclerosis, Arterioscler. Thromb. Vasc. Biol. 24 (12) (2004) 2227–2236.
[14] I. Moreno-Indias, et al., Impact of the gut microbiota on the development of obesity and type 2 diabetes mellitus, Front. Microbiol. 5 (2014) 190.
[15] F. Liu, et al., Alterations of urinary microbiota in type 2 diabetes mellitus with hypertension and/or hyperlipidemia, Front. Physiol. 8 (2017) 126.
[16] A. Spor, et al., Unravelling the effects of the environment and host genotype on the gut microbiome, Nat Rev Microbiol 9 (4) (2011) 279–290.
[17] M. Deschasaux, et al., Depicting the composition of gut microbiota in a population with varied ethnic origins but shared geography, Nat. Med. 24 (2018) 1526–1531.
[18] D. Rothschild, et al., Environment dominates over host genetics in shaping human gut microbiota, Nature 555 (7695) (2018) 210–215.
[19] C.L. Kien, et al., Increased colonic luminal synthesis of butyric acid is associated with lowered colonic cell proliferation in piglets, J. Nutr. 136 (1) (2006) 64–69.
[20] P.J. Turnbaugh, et al., An obesity-associated gut microbiome with increased capacity for energy harvest, Nature 444 (7122) (2006) 1027–1031.
[21] T.T. Macdonald, G. Monteleone, Immunity, inflammation, and allergy in the gut,

Science 307 (5717) (2005) 1920–1925.
[22] E.E. Canfora, et al., Short-chain fatty acids in control of body weight and insulin sensitivity, Nat Rev Endocrinol 11 (10) (2015) 577–591.
[23] I. Kimura, et al., The SCFA receptor GPR43 and energy metabolism, Front Endocrinol (Lausanne) 5 (2014) 85.
[24] A. Worthmann, et al., Cold-induced conversion of cholesterol to bile acids in mice shapes the gut microbiome and promotes adaptive thermogenesis, Nat. Med. 23 (7) (2017) 839–849.
[25] Y. Kusumoto, et al., Bile acid binding resin prevents fat accumulation through intestinal microbiota in high-fat diet-induced obesity in mice, Metabolism 71 (2017) 1–6.
[26] K. Takeda, et al., Toll-like receptors, Annu. Rev. Immunol. 21 (2003) 335–376.
[27] B. Beutler, Inferences, questions and possibilities in toll-like receptor signalling, Nature 430 (6996) (2004) 257–263.
[28] C.A. Thaiss, et al., The microbiome and innate immunity, Nature 535 (7610) (2016) 65–74.
[29] M. Vijay-Kumar, et al., Metabolic syndrome and altered gut microbiota in mice lacking toll-like receptor 5, Science 328 (5975) (2010) 228–231.
[30] H. Shi, et al., TLR4 links innate immunity and fatty acid-induced insulin resistance, J. Clin. Invest. 116 (11) (2006) 3015–3025.
[31] K. Honda, D.R. Littman, The microbiota in adaptive immune homeostasis and disease, Nature 535 (7610) (2016) 75–84.
[32] M. Fulde, et al., Neonatal selection by Toll-like receptor 5 influences long-term gut microbiota composition, Nature 560 (7719) (2018) 489–493.
[33] J.E. Davis, et al., Tlr-4 deficiency selectively protects against obesity induced by diets high in saturated fat, Obesity (Silver Spring) 16 (6) (2008) 1248–1255.
[34] E.E. Jackson, et al., Loss of Toll-like receptor 4 function partially protects against peripheral and cardiac glucose metabolic derangements during a long-term high-fat diet, PLoS One 10 (11) (2015) e0142077.
[35] L.A. Velloso, et al., TLR4 at the crossroads of nutrients, gut microbiota, and metabolic inflammation, Endocr. Rev. 36 (3) (2015) 245–271.
[36] L.H. Kuo, et al., Toll-like receptor 2 deficiency improves insulin sensitivity and hepatic insulin signalling in the mouse, Diabetologia 54 (1) (2011) 168–179.
[37] J.A. Ehses, et al., Toll-like receptor 2-deficient mice are protected from insulin resistance and beta cell dysfunction induced by a high-fat diet, Diabetologia 53 (8) (2010) 1795–1806.
[38] H.J. Jang, et al., Toll-like receptor 2 mediates high-fat diet-induced impairment of vasodilator actions of insulin, Am. J. Physiol. Endocrinol. Metab. 304 (10) (2013) E1077–E1088.
[39] J.E. Davis, et al., Absence of Tlr2 protects against high-fat diet-induced inflammation and results in greater insulin-stimulated glucose transport in cultured adipocytes, J. Nutr. Biochem. 22 (2) (2011) 136–141.
[40] R.W. Himes, C.W. Smith, Tlr2 is critical for diet-induced metabolic syndrome in a murine model, FASEB J. 24 (3) (2010) 731–739.
[41] A.A. Amato, et al., GQ-16, a novel peroxisome proliferator-activated receptor γ (PPARγ) ligand, promotes insulin sensitization without weight gain, J. Biol. Chem. 287 (33) (2012) 28169–28179.
[42] R.M. Bezerra, et al., A high-fructose diet induces insulin resistance but not blood pressure changes in normotensive rats, Braz. J. Med. Biol. Res. 34 (9) (2001) 1155–1160.
[43] R.A. Bagarolli, et al., Probiotics modulate gut microbiota and improve insulin sensitivity in DIO mice, J. Nutr. Biochem. 50 (2017) 16–25.
[44] M.J. Saad, et al., Regulation of insulin receptor substrate-1 in liver and muscle of animal models of insulin resistance, J. Clin. Invest. 90 (5) (1992) 1839–1849.
[45] T.M. Zanotto, et al., Blocking iNOS and endoplasmic reticulum stress synergistically improves insulin resistance in mice, Mol Metab 6 (2) (2017) 206–218.
[46] A.C. Thirone, et al., Regulation of Cbl-associated protein/Cbl pathway in muscle and adipose tissues of two animal models of insulin resistance, Endocrinology 145 (1) (2004) 281–293.
[47] M.J. Saad, et al., Regulation of insulin receptor, insulin receptor substrate-1 and phosphatidylinositol 3-kinase in 3T3-F442A adipocytes. Effects of differentiation, insulin, and dexamethasone, Mol. Endocrinol. 8 (5) (1994) 545–557.
[48] Illumina 16S metagenomic sequencing library preparation (Illumina Technical Note 15044223), https://support.illumina.com/downloads/16s_metagenomic_sequencing_library_preparation.html, (2014) (19 jun).
[49] J.C. Won, et al., Central administration of an endoplasmic reticulum stress inducer inhibits the anorexigenic effects of leptin and insulin, Obesity (Silver Spring) 17 (10) (2009) 1861–1865.
[50] V. Ramirez-Alcantara, et al., Protection from diclofenac-induced small intestinal injury by the JNK inhibitor SP600125 in a mouse model of NSAID-associated enteropathy, Am. J. Physiol. Gastrointest. Liver Physiol. 297 (5) (2009) G990–G998.
[51] D. Zhou, et al., Total fecal microbiota transplantation alleviates high-fat diet-induced steatohepatitis in mice via beneficial regulation of gut microbiota, Sci. Rep. 7 (1) (2017) 1529.
[52] C. Ubeda, et al., Intestinal microbiota containing Barnesiella species cures vancomycin-resistant Enterococcus faecium colonization, Infect. Immun. 81 (3) (2013) 965–973.
[53] N. Segata, et al., Metagenomic biomarker discovery and explanation, Genome Biol. 12 (6) (2011) R60.
[54] R.J. Barnard, et al., Diet-induced insulin resistance precedes other aspects of the metabolic syndrome, J Appl Physiol (1985) 84 (4) (1998) 1311–1315.
[55] R.J. Barnard, et al., Effects of a high-fat, sucrose diet on serum insulin and related atherosclerotic risk factors in rats, Atherosclerosis 100 (2) (1993) 229–236.
[56] R. Kellermayer, et al., Colonic mucosal DNA methylation, immune response, and microbiome patterns in toll-like receptor 2-knockout mice, FASEB J. 25 (5) (2011) 1449–1460.
[57] V. Nehra, et al., Gut microbiota: modulation of host physiology in obesity, Physiology (Bethesda) 31 (5) (2016) 327–335.
[58] L. Lahti, et al., Associations between the human intestinal microbiota, Lactobacillus rhamnosus GG and serum lipids indicated by integrated analysis of high-throughput profiling data, PeerJ 1 (2013) e32.
[59] T.W. Hoffmann, et al., Microorganisms linked to inflammatory bowel disease-associated dysbiosis differentially impact host physiology in gnotobiotic mice, ISME J 10 (2) (2016) 460–477.
[60] N. Jiao, et al., Gut microbiome may contribute to insulin resistance and systemic inflammation in obese rodents: a meta-analysis, Physiol. Genomics 50 (4) (2018) 244–254.
[61] S. Ussar, et al., Interactions between gut microbiota, host genetics and diet modulate the predisposition to obesity and metabolic syndrome, Cell Metab. 22 (3) (2015) 516–530.
[62] S. Leclercq, et al., Intestinal permeability, gut-bacterial dysbiosis, and behavioral markers of alcohol-dependence severity, Proc. Natl. Acad. Sci. U. S. A. 111 (42) (2014) E4485–E4493.
[63] X. Wei, et al., Xiexin tang improves the symptom of type 2 diabetic rats by modulation of the gut microbiota, Sci. Rep. 8 (1) (2018) 3685.
[64] N.E.S. Monteiro, et al., Dietary whey proteins shield murine cecal microbiota from extensive disarray caused by a high-fat diet, Food Res. Int. 85 (2016) 121–130.
[65] E. Cario, et al., Toll-like receptor 2 controls mucosal inflammation by regulating epithelial barrier function, Gastroenterology 132 (4) (2007) 1359–1374.
[66] E. Cario, Bacterial interactions with cells of the intestinal mucosa: Toll-like receptors and NOD2, Gut 54 (8) (2005) 1182–1193.
[67] A. Monroy, et al., Impaired regulation of the TNF-alpha converting enzyme/tissue inhibitor of metalloproteinase 3 proteolytic system in skeletal muscle of obese type 2 diabetic patients: a new mechanism of insulin resistance in humans, Diabetologia 52 (10) (2009) 2169–2181.
[68] M. Federici, et al., Timp3 deficiency in insulin receptor-haploin sufficient mice promotes diabetes and vascular inflammation via increased TNF-alpha, J. Clin. Invest. 115 (12) (2005) 3494–3505.
[69] D. Tripathy, et al., Pioglitazone improves glucose metabolism and modulates skeletal muscle TIMP-3-TACE dyad in type 2 diabetes mellitus: a randomised, double-blind, placebo-controlled, mechanistic study, Diabetologia 56 (10) (2013) 2153–2163.
[70] N. Laflamme, et al., Cooperation between toll-like receptor 2 and 4 in the brain of mice challenged with cell wall components derived from gram-negative and gram-positive bacteria, Eur. J. Immunol. 33 (4) (2003) 1127–1138.
[71] D.W. Good, et al., Toll-like receptor 2 is required for LPS-induced Toll-like receptor 4 signaling and inhibition of ion transport in renal thick ascending limb, J. Biol. Chem. 287 (24) (2012) 20208–20220.
[72] S. Ussar, et al., Interactions between host genetics and gut microbiome in diabetes and metabolic syndrome, Mol Metab 5 (9) (2016) 795–803.
[73] S. Fujisaka, et al., Antibiotic effects on gut microbiota and metabolism are host dependent, J. Clin. Invest. 126 (12) (2016) 4430–4443.
[74] M.C. Arrieta, et al., Human microbiota-associated mice: a model with challenges, Cell Host Microbe 19 (5) (2016) 575–578.